

Fundamental Models of Coal Char Formation and Combustion

R. Hurt (Robert_Hurt@brown.edu, 401-863-2685)
J. Calo (Joseph_Calo@brown.edu, 401-863-1421)
Division of Engineering, Box D
Brown University
Providence, RI 02912

C. Hadad (hadad.1@osu.edu, 614-688-3141)
R. Essenhigh (essenhigh.1@postbox.acs.ohio-state.edu, 614-292-0403)
Ohio State University
206 W. 18th Ave.
Columbus, OH 43210-1107

A. Kerstein (Kerstein@CA.Sandia.gov, 510-294-2390)
Combustion Research Facility
Sandia National Laboratories,
Livermore CA 94550

OBJECTIVE

The overall objective of this project is to carry out the fundamental research needed to develop a first-generation, structure-based model of coal char formation and combustion. Current models of char combustion and carbon burnout estimate char behavior from empirical relations based on parent coal properties. With the wide range of fuels of interest to modern combustion systems (international coals, biomass fuels, waste fuels) there is a need for more fundamental, generalized techniques to predict solid fuel char behavior.

The project involves combustion experimentation at a variety of scales, theoretical treatments of surface chemistry, and the development and refinement of advanced modeling techniques describing solid-state transformations in coal chars. The fundamental modeling approach taken here may also produce auxiliary benefits for other coal technologies, including cokemaking, liquefaction, activated carbon production and use, and carbon materials manufacture (fibers, composites, graphite, etc.). Carbon nanostructure, the size and spatial arrangement of the graphene layer segments that are the basic building blocks of carbons, plays an important role in each of these diverse applications. This combined experimental and theoretical approach will result in a first-generation, structure-based model that is a significant improvement over empirical models.

APPROACH

This project consists of the following three interrelated tasks: (1) Project Management, (2) Development of Structure-Based Models, and (3) Experiments in Practical Combustion Systems. In Task 2, dynamic models are being formulated that describe the formation and evolution of char nanostructure in flames. Also, modern computational chemistry is being used to understand the pathways for oxidative attack on model PAH and graphitic structures. This task also includes laboratory-scale experiments designed to understand thermal annealing and mineral / carbon interactions, and a direct investigation of carbon nanostructural rearrangements by *in-situ*, hot-stage HRTEM. Task 3 represents a parallel effort to investigate and document the importance

of thermal history effects on char structure and reactivity in well-controlled and characterized coal flames. Comparative experiments will be carried out on two reactor facilities with widely varying flame type and the properties and reactivities of the chars characterized.

SELECTED RESULTS

Significant progress has been made on several different fronts. The sections below provide brief overviews of the progress to date in the areas of char nanostructure, thermal annealing, and fundamental oxidative pathways.

Models of Char Nanostructure: Formation and Evolution

Many char properties depend on nanostructure — the spatial arrangement of the graphene layers that are the basic building blocks of the material [Oberlin, 1990]. In particular, the spatial rearrangement of aromatic clusters and their oligomers occurring during pyrolysis determine the initial char nanostructure and influence the surface areas and intrinsic reactivities of the chars for subsequent combustion. Carbon materials formed from condensed phase organic precursors can be grouped into two categories: anisotropic carbons, in which the graphene layers possess long range orientational order, and isotropic carbons, in which the graphene layers exhibit short range order only [Marsh and Walker, 1979]. For many organic precursors poor in oxygen and stable sulfur, nanostructural ordering occurs in the molten stage of carbonization resulting in a discotic liquid crystalline intermediate known as carbonaceous mesophase [Marsh and Walker, 1979; Gasparoux, 1979]. Three types of liquid discotic phases are depicted in Fig. 1. The solidification of carbonaceous mesophase by chemical crosslinking upon further heat treatment results in the first category of carbon materials — those with long-range orientational order and visible optical anisotropy. Carbonaceous mesophase is believed to be a discotic liquid crystal composed of nearly planar but incompletely condensed oligomers of small aromatic clusters [Lewis 1982]. This carbonization process bears some similarity to the formation of highly ordered polymer networks by thermal crosslinking of liquid crystalline monomer precursors [Clough et al., 1976].

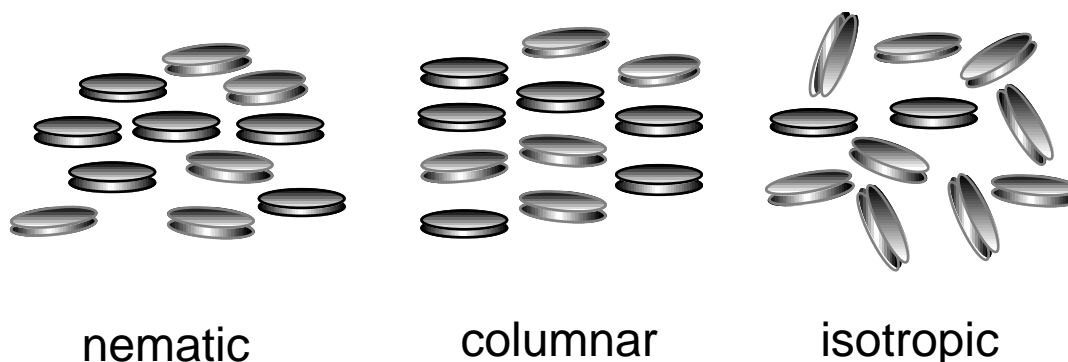


Figure 1. Liquid and liquid crystalline phases for disk-like molecules.

Carbonaceous mesophase can be formed through decreases in temperature [Lewis, 1978], or through solvent extraction which removes low molecular weight material and increases the concentration of the high molecular weight mesogens [Riggs and Diefendorf, 1980]. Carbonaceous mesophase is thus seen to have a dual thermotropic and lyotropic nature. In practice, however, carbonaceous mesophase is most commonly formed through chemical growth processes involving dehydrogenative condensation reactions between small polyaromatic clusters, producing progressively larger oligomers with near-planar geometries. In an isothermal

carbonization process, these chemical events lead to increases in mean molecular weight, which increases the effective aspect ratio of the discotic oligomers (as their thickness is nearly constant) and increases their liquid crystal forming tendency. At ~ 1000 amu a critical aspect ratio is reached and the molecules undergo a phase transition to the ordered discotic liquid crystal. Accompanying this increase in mesogen size is typically an increase in mesogen concentration, as low-molecular-weight, non-mesogenic compounds are lost by vaporization and chemical coalescence. There have been several attempts to model the formation of carbonaceous mesophase and the properties of its phase transitions using liquid crystal theory [Riggs and Diefendorf, 1980, Shishido et al., 1997, Hurt and Hu, 1998].

Isotropic carbons, comprising the second category of carbon materials, possess only short-range order, and are often formed under conditions in which the mobility of the constituent molecules is too low to allow the concerted rotational rearrangements necessary for liquid crystal formation. Indeed, many of the organic precursors that form isotropic carbons do not visibly soften or fuse upon heating — they undergo carbonization in the solid state. If solidification occurs in the isotropic state, it is not possible to introduce long range orientational order by further heat treatment. Instead, only local rearrangements occur, leading to the development of somewhat larger crystallites with nearly random orientation in a solid that is isotropic at long length scales. The development of long range order in the early stages of carbonization is thus key to the ultimate production of highly ordered graphites — this is a central concept in carbon science and underscores the importance of understanding the order transition in the early stages of carbonization [Marsh and Walker, 1979].

Recent work in this project has explored the kinetics of orientational order / disorder transitions with emphasis on highly hindered systems using simple numerical simulations. It will be demonstrated that a simple numerical model embodying the essential competition between growth rate and mobility in anisometric objects is capable of reproducing a number of key features of carbonization processes for a variety of organic precursors.

The numerical model. A simple theory was sought to describe the structural transformations occurring during the growth of anisometric objects under conditions of limited, but variable mobility. Numerical simulations were therefore conducted in which canonical anisometric objects (hard lines) grow, rotate, and translate in a two dimensional continuum. The primary advantage of the idealized geometry and reduced dimensionality is simplicity; the simulations will be shown later to be fully defined by only two dimensionless parameters, one of which has primary significance. The simulations proceed as follows. Points are chosen at random in a two-dimensional simulation box of unit length and allowed to grow into lines at a fixed rate, G , with growth occurring at both ends. The lines are also allowed to translate and rotate with mean linear and angular velocities, V and R , respectively. Random numbers are generated at each time step to determine the actual change in position and orientation for a proposed motion event. Overlap between the lines is forbidden, and thus both growth and motion are carried out in a given time step only if they do not lead to overlap. In the specific algorithm used, small growth steps alternate with small translation/rotation steps until the structure freezes into a gel and no more motion or growth is possible.

Results of the simulations are as follows. At high layer mobility, mutual avoidance causes the layers to align during the later stages of growth leading to an phase exhibiting order on a length scale comparable to the simulation box. At lower mobility / growth ratio, the alignment is hindered and the layers adopt a final state with short range order only, reminiscent of distinct crystallites with random orientation in isotropic carbon materials. These results are summarized in Figs. 2 - 4.

In Figure 2, overall order parameters for the frozen states are plotted (solid line) as a function of M^* , a dimensionless mobility to growth ratio. This figure shows a clear transition from order to disorder in a critical range of the mobility / growth ratio from 10^2 to 10^4 .

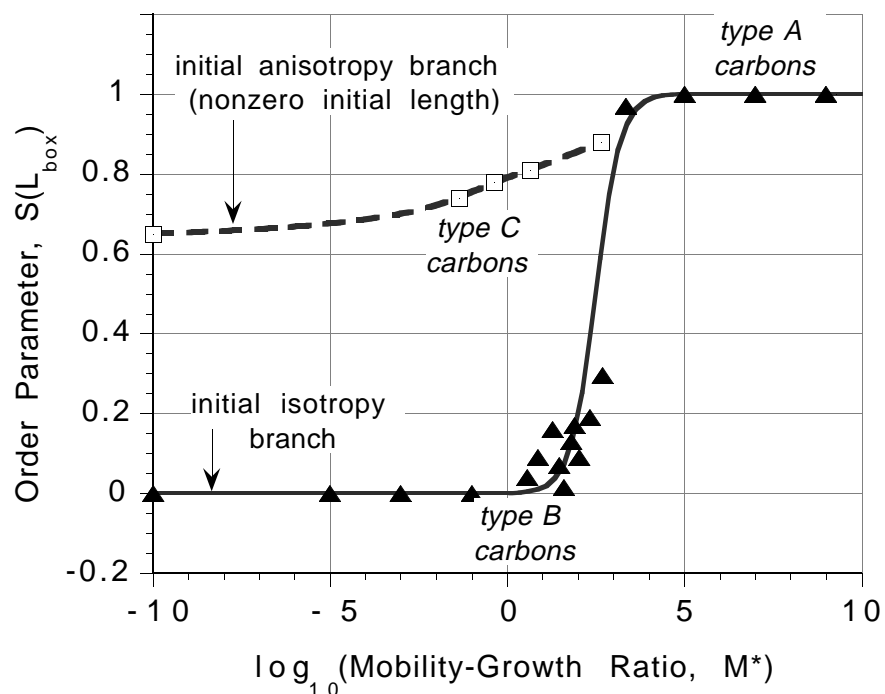


Figure 2 Summary of final states in numerical simulations starting from initially random states (isotropic parent materials) and initial ordered states (anisotropic parent materials). Long-range nematic order parameter in the final state is plotted as a function of the dimensionless mobility / growth ratio, M^* . The initially ordered states also have an initial length of $L_o/L_{box} = 0.075$. Curve labels show the relation to carbonization processes. Type A carbons: isotropic solids formed through solid-state pyrolysis (e.g from lignites, woody tissue, oxygen-rich polymers); Type B carbons: anisotropic solids formed through liquid phase pyrolysis (pitches, polyaromatic compounds, coking coals); Type C carbons: anisotropic solids formed by solid-state pyrolysis of initially ordered precursors (e.g. anthracites).

The numerical model in its simplest form is thus sufficient to distinguish two important classes of carbon materials: (1) isotropic carbons formed via all-solid-state routes in which molecular mobility is severely limited (e.g. low-rank coals, woody and cellulosic materials, and oxygen-rich thermosetting polymers such as phenol-formaldehyde resins), and (2) anisotropic carbons formed from precursors that pass through a mobile, liquid-phase intermediate (high-rank bituminous coals [Marsh, 1973], polyvinyl chloride [Marsh and Walker, 1979], anthracene [Griffin et al., 1991], many petroleum and coal-tar pitches [Greinke, 1994]).

The restrictions of zero initial length and initial order parameter are not appropriate for some carbonization processes, in particular those involving high-rank fossil fuels. Lower-rank coals with dry, ash-free carbon contents below about 85 weight-% are typically isotropic in their raw state under reflected light [Murchison, 1978]. The combination of time, temperature, and lithostatic pressure lead to an increasing aromatic cluster size and an increasing degree of orientational order parallel to the bedding plane as rank increases. High-rank bituminous coals (85 - 90 wt-% carbon, dry, ash-free) have aromatic clusters containing an average of 14 - 20 aromatic carbons as determined by NMR techniques [Smith et al., 1994], corresponding to mean molecular weights of 300 - 400 amu, including substituent groups. These clusters are only slightly larger than those in lower-rank bituminous and subbituminous coals (10-15 aromatic carbons [Smith et

al., 1994]). In each case the mean cluster size is significantly smaller than the critical molecular weight for mesophase formation (~ 1000 amu). The high-rank bituminous coals (dry, ash-free carbon $> 85\%$) show finite values of bireflectance, an measure of anisotropy computed as the difference between the minimum and maximum reflectance values when the optical stage is rotated under crossed polarizing filters [Murchison, 1978]. Anthracites, which are higher rank coals ($> \sim 92$ wt-% carbon), have larger aromatic clusters in their raw state (~ 50 aromatic carbon atoms and ~ 600 amu per cluster [Smith et al., 1994]) and show a degree of orientational order among clusters by high resolution TEM [Blanche et al., 1995], and bireflectance [Murchison, 1978].

Figure 3 show measurements of optical bireflectance as a function of carbonization temperature for three coals of various rank [Murchison, D., 1978]. These results are given as a function of temperature, rather than time, but are indicative of the solid structures observed during the various stages of carbonization, as they might occur during non-isothermal heat treatment. The lowest rank coal is isotropic in its initially state and remains essentially so during carbonization. The high-rank bituminous coal shows measurable anisotropy in its raw state, but loses this anisotropy at 400 °C, and regains it at slightly higher temperatures. Apparently the increase in mobility on heating allows the structure to relax from a metastable configuration imposed by high lithostatic pressure to a near equilibrium isotropic configuration at 1 bar pressure. As heating continues, molecular weight growth proceeds until the planar structures reach the critical size (aspect ratio) for liquid crystal formation, and a highly ordered state develops. The bireflectance thus passes through a minimum, as seen in Fig. 3 in the curve labeled high-rank bituminous. The final degree of order is very high in the sample carbonized at temperatures above 400 °C. The anthracite in raw form shows significant anisotropy, which is unaltered up to 600 °C and then slightly enhanced by higher temperature heat treatment. Despite the high degree of initial order, the anthracite does not develop the same degree of order as the high-rank bituminous coal. This is consistent with the observation that many anthracites are nongraphitizable [Blanche et al., 1995] (i.e. do not develop sufficient long range order on heating to produce graphite with good electrical and thermal properties).

To model anthracites, the basic numerical simulations were repeated with partially ordered initial states. Coordinates of the initial points were chosen randomly, as before, but initial growth directions were biased to have a preferred direction (non-zero S_0). At very low mobility, the initial orientational order in the coal is preserved intact in the char ($S = S_0$). At higher mobility, the initial order is lost, leading to isotropic final chars. At high mobilities the sample quickly loses memory of its initial order and the curve joins the previous curve for initially isotropic materials. The deep trough does not correspond to any known natural carbonaceous substance and therefore an additional factor must be added to the simple simulations to accurately simulate order development in high-rank fossil materials.

It was found that anthracitic order can be adequately represented by simulations in which the layers have a preferred initial direction (non-zero S_0) and non-zero initial length, L_0 . Indeed, TEM [Blanche et al., 1995] and NMR [Smith et al., 1994] studies of raw anthracites indicate that significant aromatic cluster development has occurred during coalification. These simulations lead to the dashed curve in Fig. 2. The simulations show a gradual, monotonic increase in final order as the mobility increases, so that anthracites produce chars with long-range order intermediate between the high-rank bituminous coals and the low-rank materials.

Finally, Fig. 4 shows *time dependent* simulation results for three cases representing important classes of carbonizing systems. The simulations show that: (1) type A precursors (e.g. low rank coals) are nearly isotropic and remain so during carbonization, (2) type B precursors (e.g. high rank bituminous coals) lose their initial anisotropy, but regain it during the latter stages of carbonization, (3) type C precursors (many anthracites) retain and slightly enhance their anisotropy during carbonization. Comparing Figs. 3 and 4, it is seen that the simple hard-line simulations also mimic these major trends seen in the bireflectance studies.

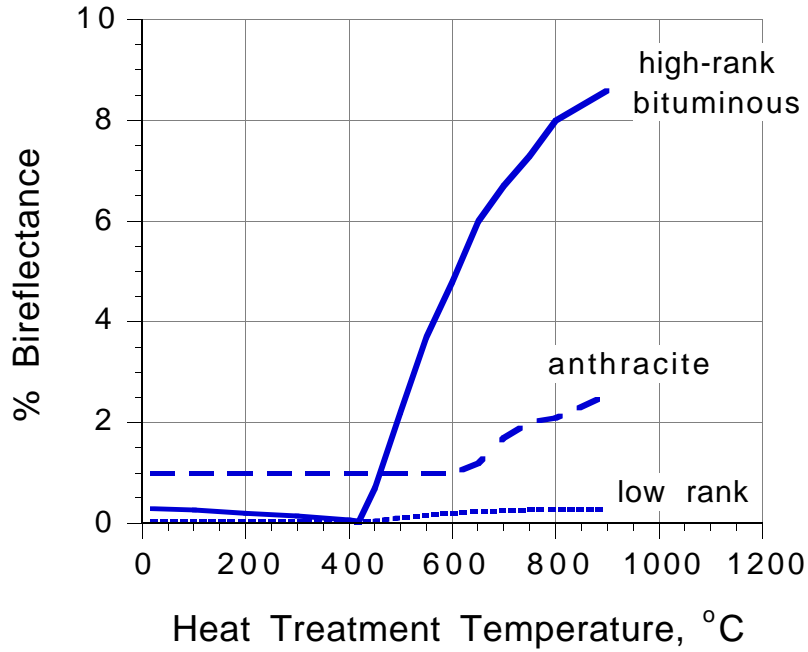


Figure 3 Measurements of optical bireflectance as a function of carbonization temperature for three important classes of coals from Murchison [1978].

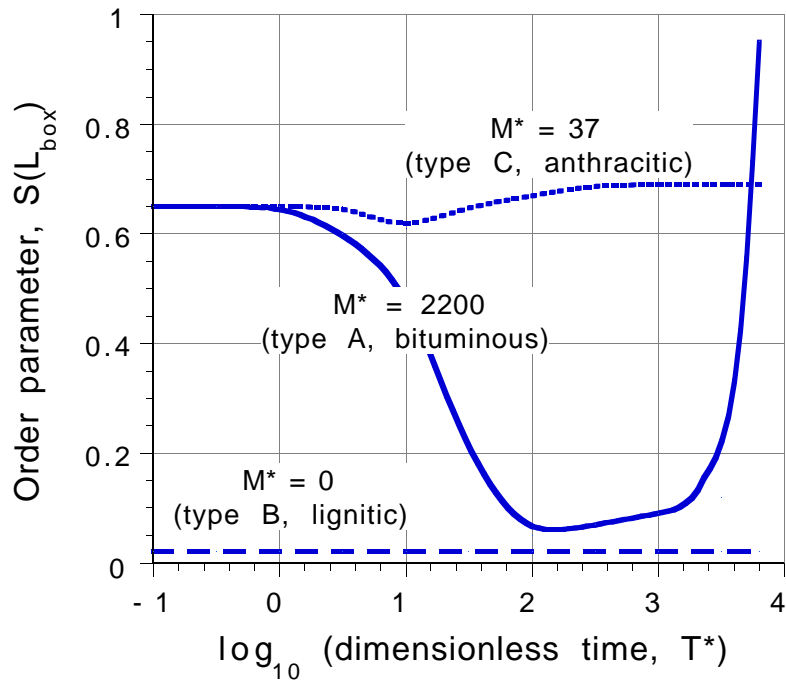


Figure 4 Simulation results: Time evolution of the long-range nematic order parameter in three simulations representing important classes of carbonization processes.

Thermal Annealing

This project has also been investigating the phenomenon of thermal annealing in chars, whereby reactivity decreases as severity of heat treatment (temperature and time) increases. Oxidation reactivity and surface areas have been measured for three coals of varying rank and for a model carbon material from phenol-formaldehyde resin as a function of heat treatment temperature and oxidative conversion. In parallel, char nanostructural evolution has been tracked using the near-atomic-resolution technique of HRTEM fringe imaging. Results indicate for most chars that higher heat treatment temperature reduces char reactivity, as expected, but that the reactivity differences diminish as oxidation proceeds, so that the reactivity of many highly burned-out chars are similar. This result has important implications for flame modelling and is being investigated further.

Fundamental Oxidative Pathways for PAH

In the area of computational chemistry, our goal is to examine the potential energy surface and mechanism of reactivity on a coal char surface so as to understand the kinetic issues involved. The approach has been to model these coal char surfaces by using polycyclic aromatic hydrocarbons (PAHs), and this report will provide more information towards this goal. Recently work has focused on specific sites of hydrogen atom abstraction of model PAHs (i.e. the preference for bond dissociation and the beginning of reactivity), the bond dissociation energies of larger PAHs (see Fig. 5), and the mechanism of oxidative decomposition of monocyclic rings. Theoretical analyses have also been carried out examining the dissociative and nondissociative forms of the adsorption / desorption kinetic schemes used to describe high-temperature char combustion [Klimesh and Essenhigh, 1998].

This project has provided evidence for the accurate treatment of the reactivity of graphitic surfaces by density functional theoretical methods. In particular, we have shown that the “hybrid” B3LYP method can be used to provide quantitative information on the stability of the corresponding radicals that arise from hydrogen atom abstraction from monocyclic aromatic rings. We have continued to explore the potential energy surfaces for oxidative decomposition of aromatic radicals with oxygen. We are particularly interested in the intermediates involved in the combustion process and the requirements for efficient reactivity of a coal char. Morokuma and Lin have recently published calculations on the vinyl radical with O₂ using B3LYP geometries. They have also published calculations in the past few years on intermediates of relevance to the oxidation of benzene. Their results suggest that the B3LYP method provides results which are in good qualitative and quantitative agreement with higher levels of theory on the potential energy surfaces.

Previously, we reported preliminary potential energy surfaces for the O₂ chemistry of radicals derived from benzene and furan (at the C-2 position only). We have continued with these projects and have also added pyridine to our study. We are particularly interested in the mode of decomposition of these radical intermediates so as to provide the bottle-necks for oxidation on a coal char surface.

Example potential energy surfaces are provided as Figure 6 (furan at C-2) and Figure 7 (furan at C-3). In our calculated mechanisms, we have chosen to explore intermediates in the oxidation of these radicals according to a mechanism proposed by Barry Carpenter [1993] using semi-empirical MO theory. The thermodynamic energy changes for the phenyl radical with O₂ system to proceed from one intermediate to another with eventual CO₂ production. Indeed, the initial adduct formation with O₂ is exothermic by about 45 kcal·mol⁻¹ and most steps thereafter are significantly exothermic or slightly endothermic. This value is very similar to that reported for the adduct of O₂ with the vinyl radical (from H-atom abstraction on ethylene) [Mabel et al., 1996]. These results would suggest that the overall rate of benzene oxidation might be limited by the initial formation of the phenyl radical and the stabilization of the O₂ adduct. Indeed, Morokuma, Lin and coworkers have shown that the reaction of vinyl radical with O₂ is dominated by the stabilization of the adduct.

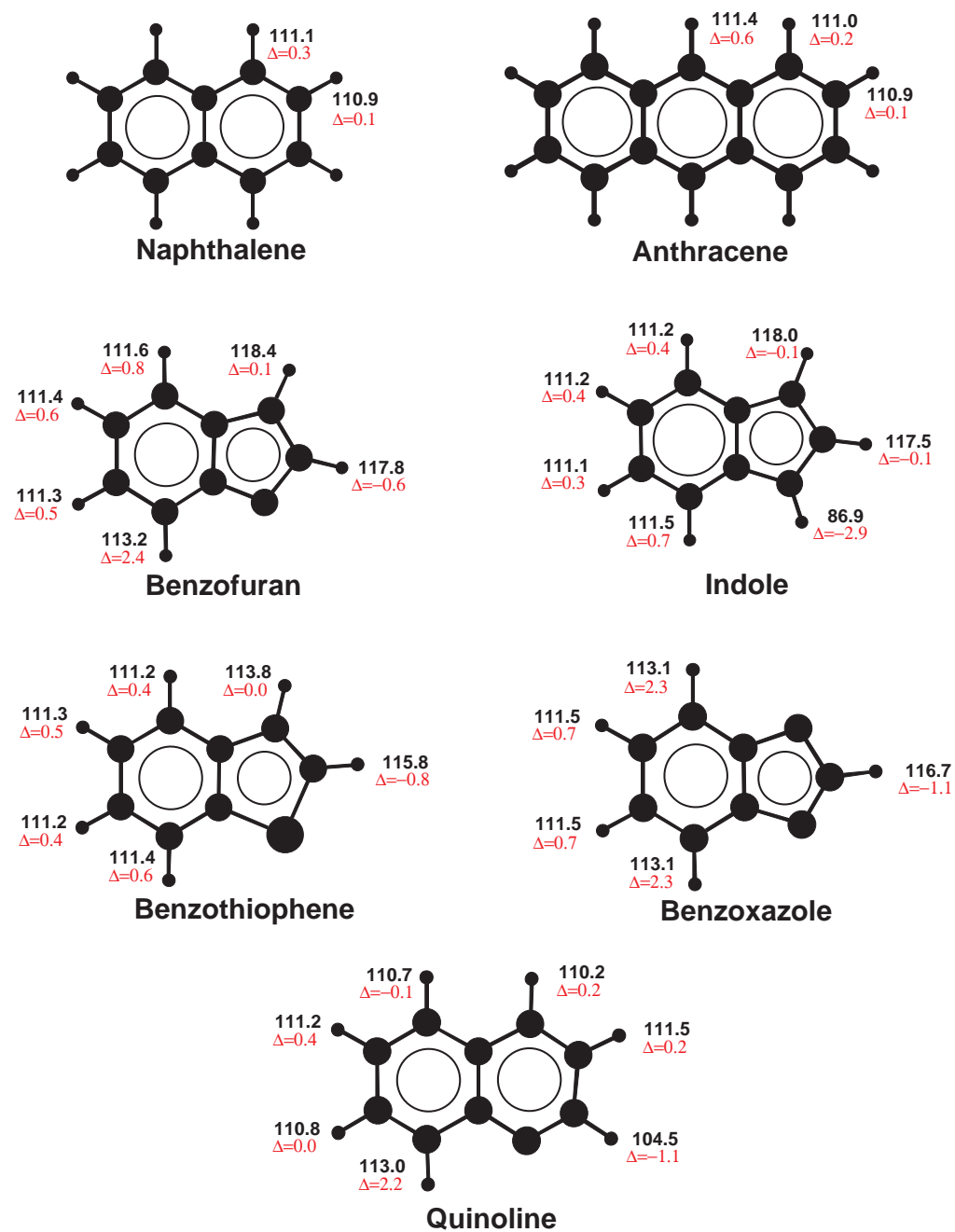


Figure 5. Bond dissociation energies for polycyclic aromatic hydrocarbons.

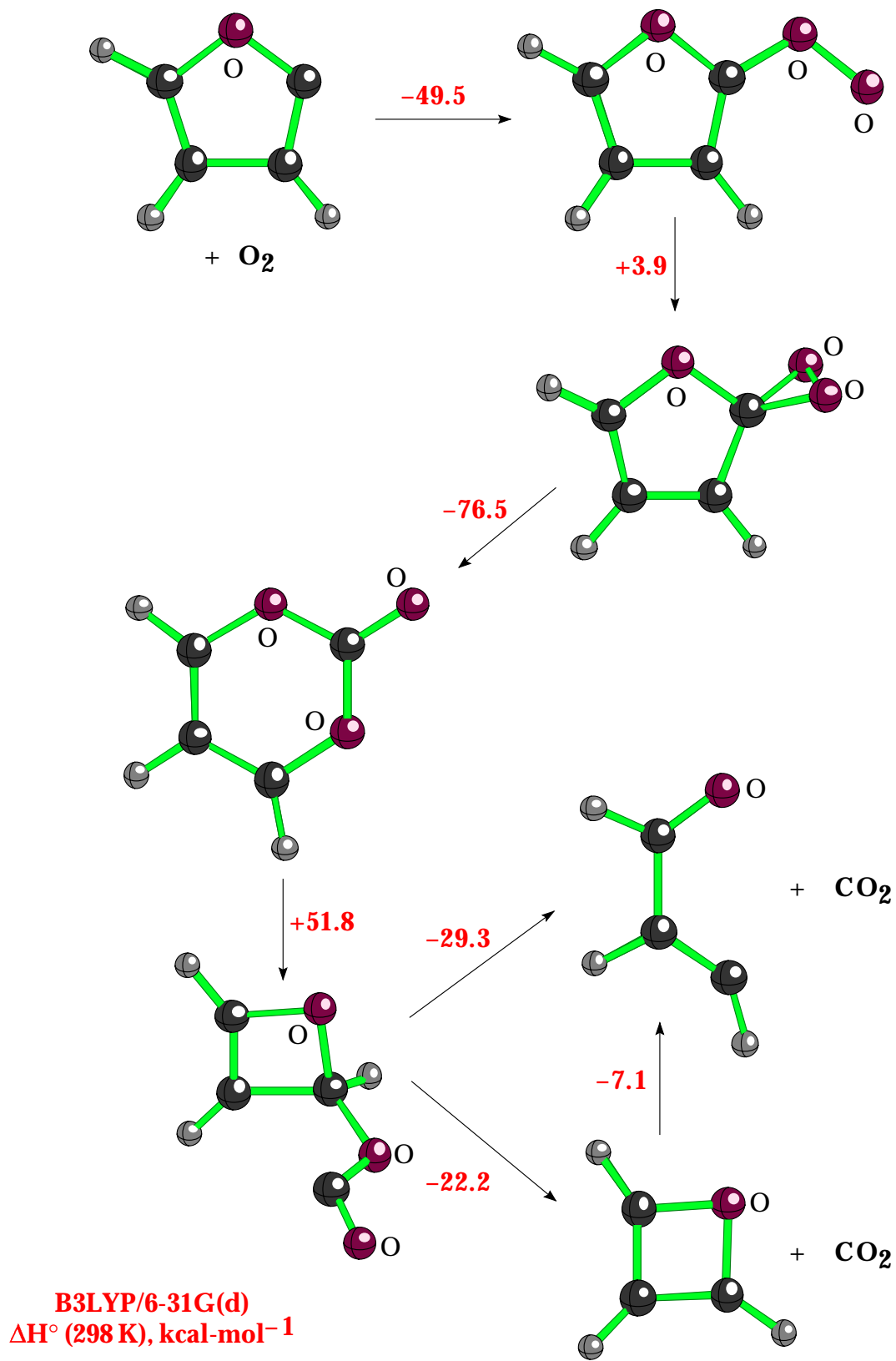


Figure 6. Mechanism of oxidation for the 2-furanyl radical.

OXIDATION OF 3-FURANYL RADICAL
B3LYP/6-31G*

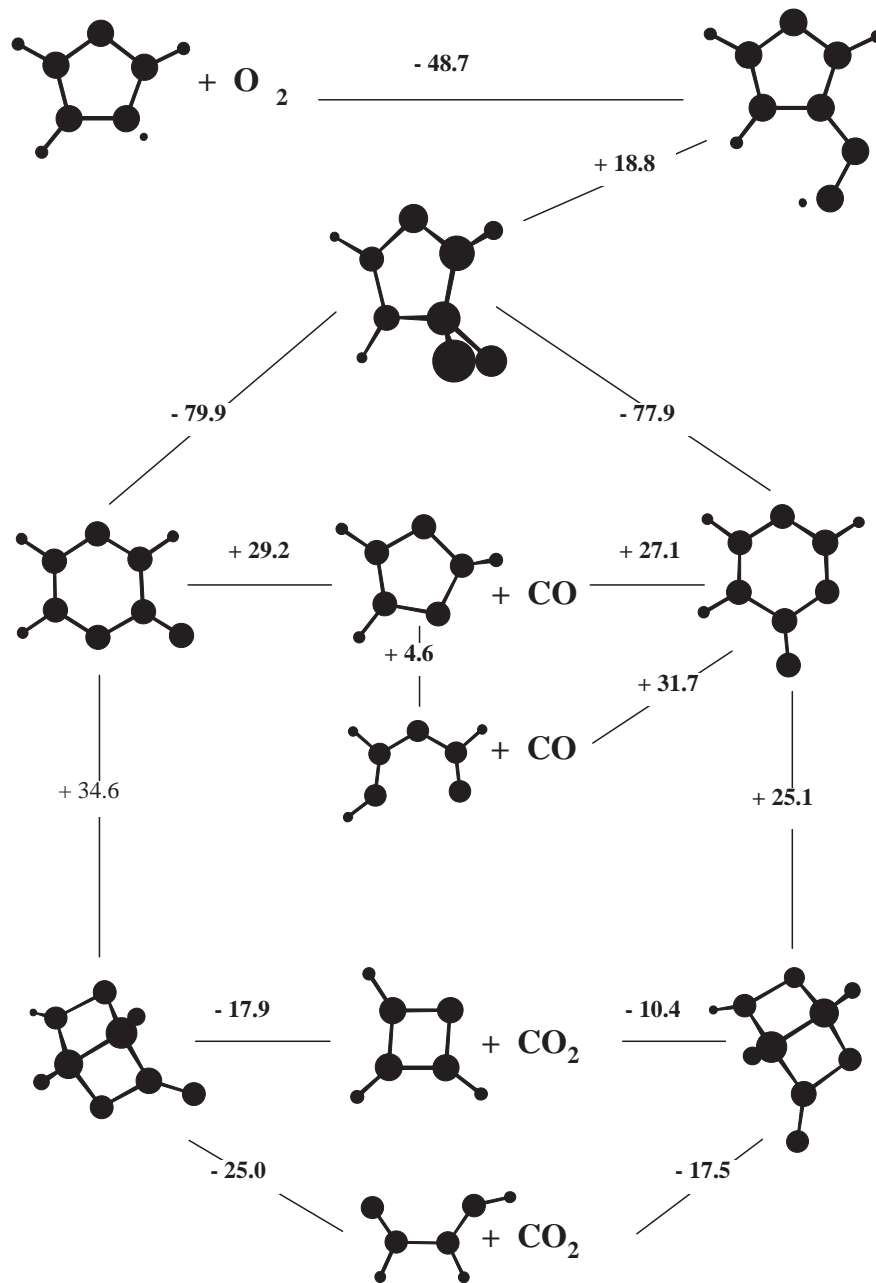


Figure 7. Mechanism of oxidation for the 3-furanyl radical.

Furan and pyridine present additional problems as there are more than one unique site of H-atom abstraction. We have proceeded to examine the oxidation of furan at the B3LYP/6-31G(d) level (see Figures 6 and 7). The surfaces look very similar to that for phenyl radical. The initial adduct with O₂ is exothermic by about 49 kcal·mol⁻¹. Opening of the 5-membered ring to a 6-membered ring with a carbonate functionality is very favorable. We have found two different avenues for CO₂ formation as well as routes for CO generation.

Pyridine shows many of the same trends. The initial addition of O₂ is very exothermic (−43 kcal·mol⁻¹) and similar structural modifications follow that initial exothermic reaction. We have determined pathways for the evolution of CO, CO₂ and HCN as products. Due to the large initial exothermic addition of O₂, we expect that the oxidation of pyridine will be limited to initial formation of the pyridyl radical. We are continuing on our search for intermediates for the other positions of pyridine. Previously we also presented preliminary results on the radical formation step with these simple aromatic compounds. We have found that the potential energy surfaces for H-atom abstraction by H, OH, O (³P), and O₂ are actually quite complicated, and we will present more information in our next quarterly report.

For the near future, we will continue to explore the hydrogen atom abstraction step for monocyclic and larger PAHs. We will also continue to probe the O₂ mechanism for oxidation of benzene and other PAHs that was recently postulated by Carpenter. We have extended this study to pyridine, and we will also examine the chemistry of thiophene. We hope to further explore how O₂ adds to PAHs and contributes to the size distribution of the resulting coal chars. Experimentally we will continue to explore the coal char samples and examine the chemical composition of the coal chars as provided by Professor Essenhigh. Such an experimental characterization may provide tremendous insight into the reactivity of the coal chars.

Experiments in Practical Combustion Systems. The experimental work with contrasting flame types has focused on the retrofit and refurbishing of experimental apparatus, including a high intensity tower furnace and jet mixed reactor at Ohio State. Experimental work has begun in the high intensity reactor, in which chars are prepared under rapid heating sub-stoichiometric conditions, and sampled as a function of residence time for post-combustion characterization. Major results from this task are pending.

FUTURE ACTIVITIES

The computational chemistry task will continue to explore reaction pathways with emphasis on larger aromatic systems as models of graphene layers in disordered chars. The experimental work on char formation and evolution in contrasting flame types will continue. The task on modelling char nanostructure will focus on the remaining problem of isotropic coke, an important class of carbons in combustion applications. Work will then proceed to the establishment of structure / property relations — models that relate carbon nano-, micro- and macro-structure to key properties, such as reactivity, surface area, pore structure, and burnout behavior.

CONTRACT INFORMATION AND ACKNOWLEDGMENTS

The authors would like to acknowledge financial support from the U.S. Department of Energy, Federal Energy Technology Center under contract DE-FG22-96PC96249, as well as support for Alan Kerstein by the DOE Office of Basic Energy Sciences. FETC project manager: Phil Goldberg, DOE FETC PO Box 10940 MS 922-342C, Pittsburgh, PA; 412-892-5806, Philip.Goldberg@fetc.doe.gov).

REFERENCES

- Bates, M.A., Luckhurst, G.R. *J.Chem. Phys.* 104 (17) 6696 (1996).
- Barrall, E.M., Ch. 9 in *Liquid Crystals: The Fourth State of Matter*, (Saeva, ed.), Marcel Dekker, Inc. New York, 1979.
- Blanche, C., Dumas, D., Rouzaud, J.N. *Coal Science* (Pajares and Tascon Eds.) Elsevier Science, Amsterdam, 1995, p. 43.
- Carpenter, B. K. *J. Am. Chem. Soc.* 115, 9806 (1993).
- Chandrasekhar, S., *Liquid Crystals, Second Edition*, Cambridge University Press, Cambridge, 1992.
- Clough, S.B., Blumstein, A., Hsu, E.C., *Macromolecules* 9 123 (1976).
- De Gennes P.G., Prost, J., *The Physics of Liquid Crystals*, Clarendon Press, Oxford, 1993.
- Frenkel D., Mulder, B.M. *Mol. Phys.* 55 1171-92 (1985).
- Gasparoux, H., *Mol. Cryst. Liq. Cryst.* 63 231-248 (1981).
- Gay, J.G., Berne, B.J., *J. Chem. Phys.* 74(6) (1981).
- Greinke, R.A., in *Chemistry and Physics of Carbon*, Vol. 24, Marcel Dekker, New York, 1994, p. 1.
- Griffin, R.R., Scaroni, A.W., Walker, P.L.Jr. *Carbon* 29 (7) 991 (1991).
- Hicklas, K., Bopp, P., Brickmann, J., *J.Chem. Phys.*, 101 3157-3171 (1994).
- Hurt, R.H., Hu, Y. "Thermodynamics of Carbonaceous Mesophase", *Carbon*, in press, 1998.
- Klimesh H.E., Essenhigh, R.H., Non-Dissociative and dissociative Adsorption of oxygen on Carbon: A Theoretical Comparison, to appear in the 27th Symp. (International) on Combustion, The Combustion Institute, Pittsburgh, 1998.
- Lee, S.H., Kim, H.S., Pak, H., *J. Chem. Phys.* 97 (9) 6933 (1992).
- Lewis, I.C., *Carbon* 16 503 (1978).
- Lewis I.C., *Carbon* 20 (6) 519 (1982).
- Mebel, A. M.; Diau, E. W. G.; Lin, M. C.; Morokuma, K. *J. Am. Chem. Soc.* 118, 9759 - 9771 (1996).
- Maier, W., Saupe, A.Z., *Naturforsch.* A13 564 (1958).
- Marsh, *Fuel*, 52 305 (1978).
- Marsh, H., and Walker, P.L.Jr., Chap. 3 in *Chemistry and Physics of Carbon, Vol. 15*, (Walker and Thrower, eds.) Marcel Dekker, New York, 1979.
- Murchison, D.G., Chap. 31 in *Analytical Methods for Coal and Coal Products*, Academic Press, New York, 1978.
- Oberlin, A. in *Chemistry and Physics of Carbon*, Vol. 22, Marcel Dekker, New York, 1990.
- Onsager, L., *Ann. NY Acad. Sci.* 51 627 (1949).
- Patrick, J.W., Reynolds, M.J., and Shaw, F.H., *Fuel* 52 198-204 (1973).
- Rand B. in *Handbook of Composites, Vol 1: Strong Fibers*, (Watt and Perov, eds), North-Holland, Amsterdam, 1985, p. 495.
- Riggs, D.M., Diefendorf, R.J., *Carbon '80 Baden Baden* (Deutsche Keramische Gesellschaft), 1980, pp. 326-329.
- Rouzaud, J.N., Oberlin, A., Chap. 17 in *Advanced Methodologies in Coal Characterization*, Elsevier, Amsterdam, 1990.
- Shim, H.S., Hurt, R.H., Yang, N.Y.C. "A Methodology for Analysis of 002 LF Fringe Images and its Application to Combustion-Derived Carbons", submitted to *Carbon*, 1998.
- Shishido, M., Inomata, H., Arai, K., Saito, S., *Carbon* 35(6) 797 (1997).
- Smith K.L., Smoot, L.P. Fletcher, T.H., Pugmire, R.J., *The Structure and Reaction Processes of Coal*, Plenum Press, NY, 1994.
- Solomon, P.R., Best, P.E., Yu Z.Z., and Charpenay, S. *Energy and Fuels*, 6 143 (1992).
- Suuberg, E.M., M. Wojtowicz, and J.M. Calo, *Carbon* 27, 431 (1989).